Angular intensity distribution of multiphoton-excited fluorescence from a spherical particle: geometric optics approach

A.A. Zemlyanov, Yu.E. Geints, and E.K. Panina

Institute of Atmospheric Optics,
Siberian Branch of the Russian Academy of Sciences, Tomsk

Received July 30, 2004

The angular distribution of spontaneous fluorescence excited by laser radiation inside a spherical particle is considered. The position and the effective volume of fluorescence sources emitting in the particle are calculated numerically as functions of the particle radius in the case of one-, two-, and three-photon-excited fluorescence. Within the framework of the geometric optics, an equation is derived for the mean brightness of fluorescence from the front and rear particle hemispheres. It is shown that if the fluorescence source is located near the dark hemisphere, asymmetry arises in the angular distribution of spontaneous fluorescence in the forward/backward directions, and this asymmetry becomes more pronounced with the increasing number of photons involved in the process.

Investigations aimed at development of new physical methods for diagnostics of aerosol media are of increasing interest nowadays. To improve the existing diagnostic capabilities of fluorescent techniques, it is important to consider theoretically the issues concerning the establishment of relations between characteristics of the observed fluorescent signal and the physical-chemical parameters of aerosol particles. The investigation of angular characteristics of multiphoton-excited fluorescence (MEF) in microparticles is one of such issues.

The process of multiphoton excitation of fluorescence was studied experimentally, for example, in Ref. 1. The experiments were conducted with ethanol ($m = 1.36 + i \cdot 10^{-6}$) and methanol ($m = 1.325 + i \cdot 10^{-6}$) drops of (35 ± 5) μm in radius, containing coumarin 510 dye, under the exposure to Ti:Sapphire laser radiation. The duration of laser pulses was ~100 fs. The use of such ultrashort laser pulses allowed obtaining rather high pump intensities needed for exciting spontaneous fluorescence, as well as preventing the appearance of competitive processes, for example, the stimulated Brillouin scattering. For one-, two-, and three-photon excitation of microdrops, central wavelengths of 400, 850, 1200 nm, respectively, were used. An effect was discovered, in which the spontaneous fluorescence peak was observed in the backward direction with respect to the direction of incident radiation from the pump source, and the peak magnitude increased with the increasing number of photons involved in the process (Fig. 1). In Ref. 1, this effect was explained by the capability of a spherical particle to concentrate the energy of the incident wave in its volume, as well as by the principle of reciprocity of light ray trajectories, known from theory of optical and radar systems.[2]

The objectives of this work were the qualitative consideration of the effect discovered in Ref. 1, determination of the spatial position and power of the sources of spontaneous fluorescence inside the particle based on numerical simulation, and assessment of the angular asymmetry of microparticle fluorescence within the framework of geometric optics.

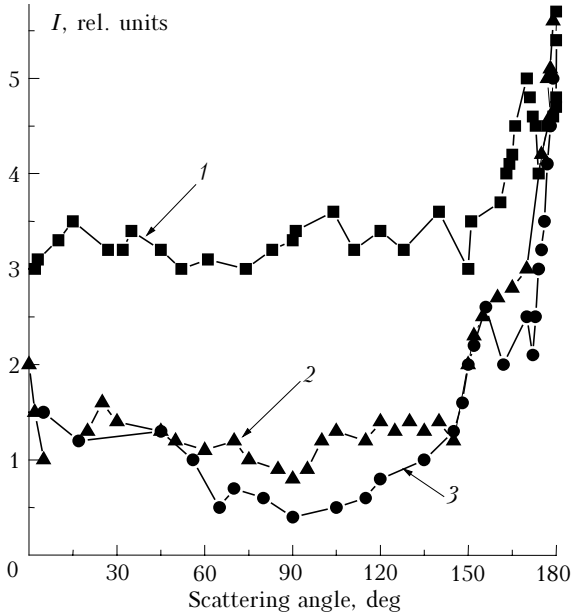

Fig. 1. Angular intensity distribution in the case of one- (*1*), two- (*2*) and three-photon-excited (*3*) fluorescence in ethanol (*1*, *2*) and methanol (*3*) drops containing coumarin 510 [Ref. 1].

In the general case, angular behavior of inelastic scattering intensity (fluorescence beyond the particle can be, probably, classified as a sort of inelastic scattering) can be deduced from solution of the integro-differential equation for the strength of the fluorescence electromagnetic field, as was done, e.g., in Refs. 3 and 4 for SRS in a microparticle.

0235-6880/04/10 737-05 $02.00

Within the framework of this approach, the electric field of nonlinearly scattered radiation $\mathbf{E}_s(\mathbf{r}; t)$ at the observation point with the radius-vector $\mathbf{r}$ can be represented in the following form:

$$\mathbf{E}_s(\mathbf{r};t) \cong \frac{k^2(\varepsilon_a - 1)}{4\pi r}\exp\{-ikr\}\times$$

$$\times \int_{V_a} \mathbf{E}_s(\mathbf{r}';t - r/c)\exp\{ikr'\cos\theta\}\mathrm{d}\mathbf{r}', \qquad (1)$$

where $k = \omega_s/c$ is the wave number of the scattered field at the frequency ω_s in the free space, ω_s is the frequency of the inelastic scattering wave; ε_a is the particle permittivity; $\mathbf{r}'$ is the radius-vector of a point inside the particle; θ is the angle between $\mathbf{r}$ and $\mathbf{r}'$. The integration is performed over the particle volume V_a.

Then the wave equation for the stimulated scattering field inside the particle, $\mathbf{E}_s(\mathbf{r}'; t)$, is considered and expanded in a series in terms of the eigenfunctions of the particle–resonator $\mathbf{E}_n(\mathbf{r})$ with the frequencies ω_n. The resultant system of algebraic equations for the expansion coefficients of the incident and nonlinearly scattered waves $\mathbf{E}_s = \sum_n A_n(t)\mathbf{E}_n(\mathbf{r})$ has the form

$$A_n\left(\omega_n^2 - \omega_s^2 + 2i\Gamma_n\omega_s\right) = \frac{4\pi}{\varepsilon_a}\omega_s^2 \int_{V_a} \mathbf{E}_n^*(\mathbf{r}')\cdot\mathbf{P}_N(\mathbf{r}')\mathrm{d}\mathbf{r}'. \qquad (2)$$

Here $\mathbf{P}_N$ is the nonlinear polarization of the medium, attributed to the studied effect of nonlinear scattering; Γ_n is the coefficient of mode damping due to the loss for absorption in the particulate matter. The integral in the right-hand side of this equation accounts for the spatial overlapping of each eigenmode in the expansion of the scattered wave field with the pump field of the nonlinear process inside the particle. The more pronounced is the overlapping, the more active is excitation of the mode of the nonlinear scattering field.

The equation (2) for the coefficients A_n along with Eq. (1) allow us to write the equation for the strength of the external field of inelastic scattering from the particle:

$$\mathbf{E}_s^{sc}(\mathbf{r};t) \cong \frac{k^2(\varepsilon_a - 1)}{\varepsilon_a r} e^{i(\omega_s t - kr)} \sum_n L_n S_n \mathbf{J}_n(\mathbf{r}_\perp). \qquad (3)$$

Here $\mathbf{r}_\perp$ is the transversal component of the radius-vector;

$$L_n = \omega_s^2/(\omega_n^2 - \omega_s^2 + 2i\Gamma_n\omega_s)$$

is the function accounting for the resonant profile of eigenmode;

$$S_n = \int_{V_a} \left(\mathbf{E}_n^*(\mathbf{r}')\cdot\mathbf{P}_N(\mathbf{r}')\right)\mathrm{d}\mathbf{r}'$$

is the integral of spatial overlapping between the fields of the eigenmode and the source of nonlinear scattering inside the particle, and the functions

$$\mathbf{J}_n(\mathbf{r}_\perp) = \int_{V_a} \left[\mathbf{r}'\times\mathbf{E}_n\right] e^{ikr'\cos\theta}\mathrm{d}o'$$

give the angular behavior of the scattered field; $\mathrm{d}o'$ is the element of the solid angle. Note that after integration these functions can be expressed through vector spherical harmonics, that is,

$$\mathbf{J}_n(\mathbf{r}_\perp) = b_n(ka_0)\left[\mathbf{r}\times\mathbf{M}_n(\mathbf{r})\right], \qquad (4)$$

where $b_n(ka_0)$ are the coefficients expressed through the integrals of the combination of spherical Bessel functions and their derivatives.[5]

Upon transition from the scattered wave field strength to its intensity

$$I_{RS}(\mathbf{r}) = c\sqrt{\varepsilon_a}/8\pi\left\langle \mathbf{E}_s(\mathbf{r})\cdot\mathbf{E}_s^*(\mathbf{r})\right\rangle$$

and the use of the polarization equation,[6] we obtain the following equation for the intensity of the scattered wave of fluorescing medium in the far zone:

$$I_{RS}(\mathbf{r}) = \frac{ck^4(\varepsilon_a - 1)^2}{8\pi\varepsilon_a^2 r^2}\sum_n\sum_m \left(L_n L_m^*\right) S_{nm}\left[\mathbf{J}_n(\mathbf{r}_\perp)\cdot\mathbf{J}_m^*(\mathbf{r}_\perp)\right], \qquad (5)$$

where the overlapping integrals

$$S_{nm} = \int_{V_a} \left[\mathbf{E}_n^*(\mathbf{r}')\cdot\mathbf{E}_m(\mathbf{r}')\right]\cdot\left[\mathbf{E}_L(\mathbf{r}')\cdot\mathbf{E}_L^*(\mathbf{r}')\right]^p \mathrm{d}\mathbf{r}'$$

are written for the field intensities; p is the number of photons involved in absorption.

The analysis of Eq. (5) shows that, in the general case, the angular intensity distribution of spontaneous multiphoton fluorescence from a spherical particle is characterized by a complex function formed by the contribution of all modes to the expansion of the field inside the particle. The contribution of each mode to the total intensity is determined by two main factors: separation of the eigenmode from the frequency of the nonlinear process and the magnitude of overlapping of the mode spatial profiles and the source field for the nonlinear scattering wave, which, in turn, depends on the corresponding degree of the pump field spatial distribution inside the particle for the p-photon process.

Thus, to calculate the angular behavior of the fluorescence field beyond the particle, it is important to know its internal optical field distribution in order to find the most intense sources of fluorescence.

As an example, Fig. 2 shows the spatial profile of the pump field relative intensity

$$B_L = \left(\mathbf{E}_L\cdot\mathbf{E}_L^*\right)/E_0^2$$

in the principal cross section of the ethanol drop with the radius $a_0 = 10$ μm, where E_0 is the electric field strength of the incident radiation, E_L is the pump field strength inside the particle. The particle is exposed to a plane wave with $\lambda = 0.8$ μm. This figure also shows analogous plots for B_L^2 and B_L^3, representing

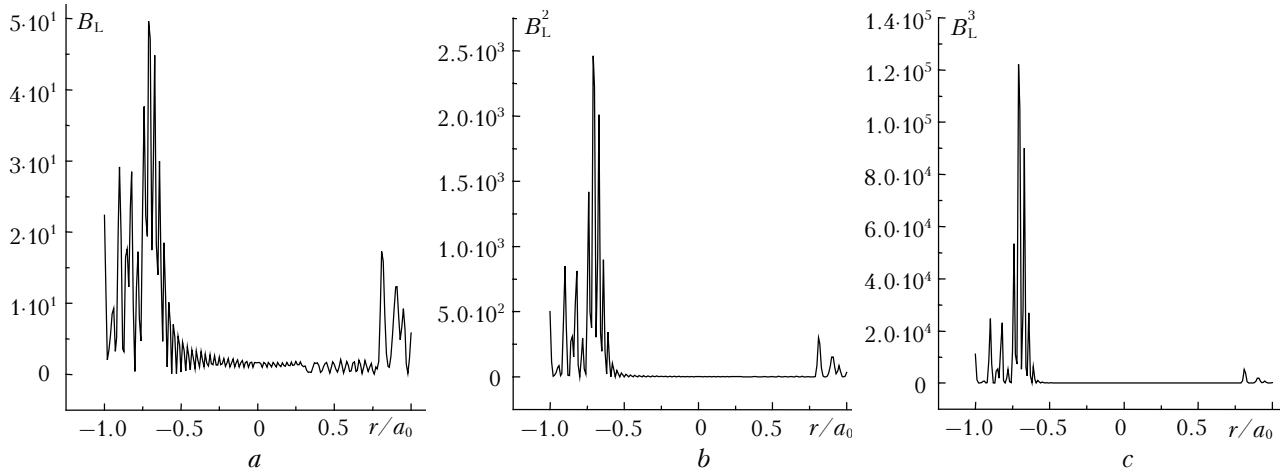

Fig. 2. Radial distribution of the internal optical field in ethanol drop (refractive index $n_1 = 1.36$) with the radius $a_0 = 10$ μm exposed to the radiation with $\lambda = 0.8$ μm in the cases of one- (*a*), two- (*b*), and three-photon (*c*) absorption. The incident radiation is directed from the right.

the intensity function of the source for the processes of two- and three-photon absorption, respectively. Since the spontaneous fluorescence is excited by the incident wave field, we can suppose that the spatial distribution of the fluorescent field in the particle will be similar to that shown in Fig. 2.

Numerical calculation of the intensity at the multiphoton excitation of fluorescence in a spherical particle is quite complicated and cumbersome; therefore, from here on, to obtain simple estimates of the effect under consideration, we will use the geometric-optics approximation.

Consider the problem of a secondary source emission in a spherical particle in the following formulation. Let the emitting source be located in the dark hemisphere of the particle at some distance b from its center along the principal diameter (Fig. 3).

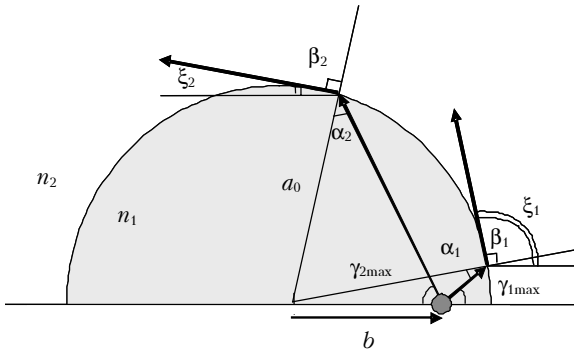

Fig. 3. Geometry of the problem about the secondary source emission in a spherical particle.

Within the framework of the proposed model, we consider only single reflection and refraction of rays at the interface between optical media. The refractive index of the particle n_1 is greater than that of the medium n_2, and, consequently, the real value of the refractive angle β of the ray emitted by the secondary source will be obtained only for the angles of incidence α so that the following condition is fulfilled:

$$\sin\alpha \le \sin\alpha_{\max} = n_2/n_1. \qquad (6)$$

For large α, a total internal reflection takes place. Using the law of sines for triangles

$$\sin\alpha = \sin\gamma\,(b/a_0) \le \sin\alpha_{\max}$$

and Eq. (6), we obtain the condition imposed on the limiting angle $\gamma_{\max}$ of ray departure from the source, at which the emitted ray still leaves the particle:

$$\gamma_{\max} = \arcsin\left(\frac{n_2}{n_1}\frac{a_0}{b}\right). \qquad (7)$$

Figure 4 shows the ray path geometry in a particle of an arbitrary radius. It can be seen that if the source lies on the optical axis near the dark surface, then some rays, for which $\alpha > \alpha_{\max}$, are reflected from the particle surface, forming so-called "whispering gallery modes." Other rays, refracting at the surface, are scattered in different directions. As the source displaces to the center, the zone O_1O_2 narrows, and, as follows from Eq. (7), at $b = (n_2/n_1)a_0$ only one ray is subject to the total internal reflection.

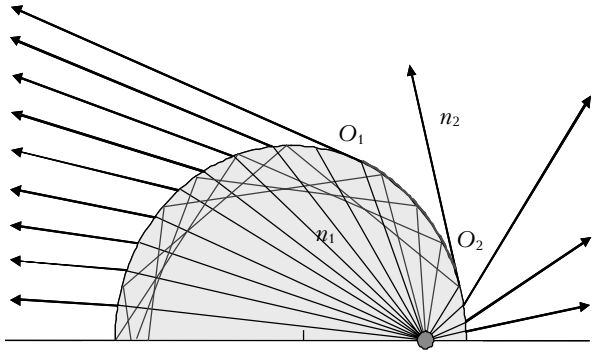

Fig. 4. Ray path geometry for the emitting source located in the rear hemisphere of a spherical particle.

In the case of fluorescence induced by one-photon absorption, the radiation source is formed not only in the dark, but also in the light hemisphere of the

particle (see Fig. 2). The ray path geometry for this source is reflection-similar to the geometry shown in Fig. 4. For one-photon absorption, because the intensities of the emitting sources are of the same order of magnitude, the phase function of the scattered radiation is close to symmetric. A quite different pattern is observed for multiphoton processes. It follows from Fig. 2 that already at $p = 2$ the nonlinear absorption occurs mostly only in the zone of the absolute maximum of intensity of the internal field located near the particle's dark surface, and, consequently, just this source is the main contributor to the total scattering.

It can be easily shown that the limiting angles of departure of rays γ_{max} from the source inside the particle in the forward and backward directions are identical ($\gamma_{1max} = \gamma_{2max}$). Therefore, for isotropic radiation, powers emitted into the rear and front hemispheres of the particle are identical ($P_1 = P_2$). However, because the secondary emission source is shifted about the particle's center, the rays leaving the particle are refracted at the surface and scattered in the forward and backward directions at different angles. This leads to different magnitudes of the spontaneous emission mean brightness $\bar{J}$ in these directions.

Using Eq. (7) for the limiting angle of departure of rays from the source, we obtain the equations for the angles of maximal deflection of edge rays in the forward direction

$$\xi_1 = \frac{3}{2}\pi - \left\{\arcsin\left(\frac{n_2}{n_1}\right) + \arcsin\left(\frac{n_2}{n_1}\frac{a_0}{b}\right)\right\}$$

and backward direction

$$\xi_2 = \arcsin\left(\frac{n_2}{n_1}\right) + \arcsin\left(\frac{n_2}{n_1}\frac{a_0}{b}\right) - \frac{\pi}{2}$$

beyond the particle with respect to the direction of the principal optical axis (angles ξ_1 and ξ_2 in Fig. 3).

The fluorescence mean brightness far from the particle will be determined as a ratio of the total power of fluorescence from the source into a hemisphere to the corresponding limiting angle of the radiation departure from the particle:

$$\bar{J}_{1,2} = P_{1,2} / \xi_{1,2},$$

where subscripts 1 and 2 correspond to the rear and front hemispheres, respectively. Then, the ratio of the mean fluorescent brightness in the forward/backward directions is

$$\bar{J}_1 / \bar{J}_2 = \xi_2 / \xi_1.$$

The numerical estimation is performed for three-photon excitation of the internal optical field in the ethanol drop with a radius of 10 μm. Here $n_1 = 1.36$, $n_2 = 1$, $\alpha_{max} = 48°$, $\beta_{max} = 90°$. Taking $b/a_0 \cong 0.7$, we obtain the ratio of the mean fluorescent brightness $\bar{J}$ in the forward/backward directions equal to $\bar{J}_1/\bar{J}_2 \sim 0.2$. This result is in agreement with the conclusions of the experimental work.[1]

As was already mentioned above, unlike two- and three-photon absorption, when the local increase in the intensity of the secondary source near the dark surface is observed, the fluorescence induced by one-photon absorption is characterized by the presence of two sources with intensity maxima near the dark and light surfaces with the smoother distribution of the field. These zones are extended and displaced by 0.6–0.8 particle radius from the particle's center.

To estimate the size of these zones, we use their effective volume V_m, determined by the e^{-1} level of the factor B_L maximum in each hemisphere of the particle. The numerically calculated ratio of V_m to the total volume V_a of different-size ethanol drops for the process of one-photon fluorescence is shown in Fig. 5.

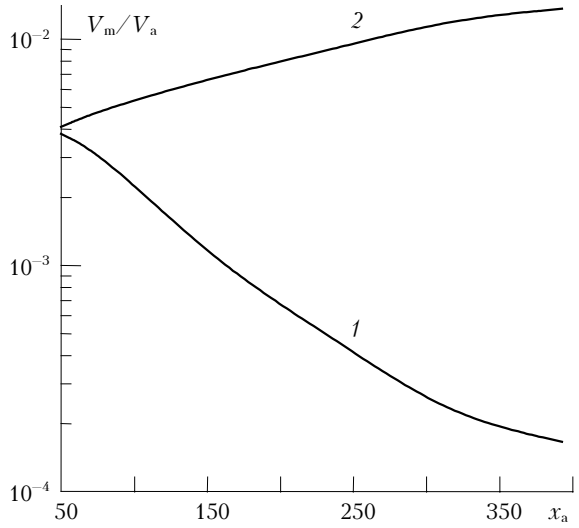

Fig. 5. Ratio of the emitting source effective volume to the ethanol drop volume as a function of the diffraction parameter $x_a = 2\pi a_0/\lambda$ for the front (*1*) and rear (*2*) maxima in the case of one-photon absorption.

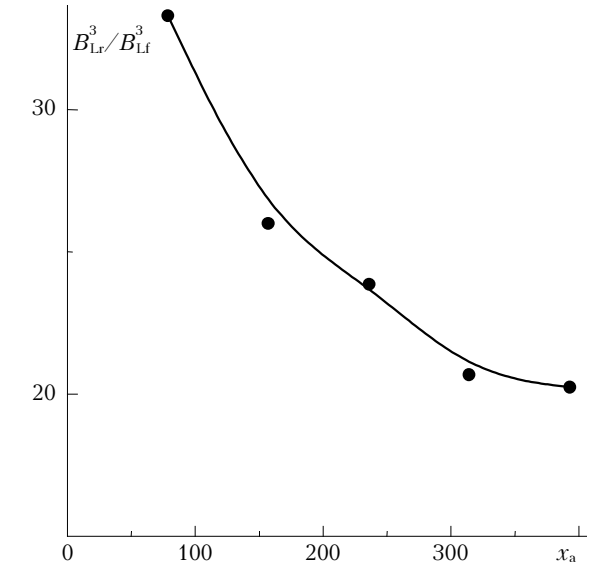

Fig. 6. Ratio of relative intensity of the pump field in the zone of the rear maximum to the front maximum B^3_{Lr}/B^3_{Lf} as a function of the diffraction parameter x_a of ethanol drop in the case of three-photon absorption.

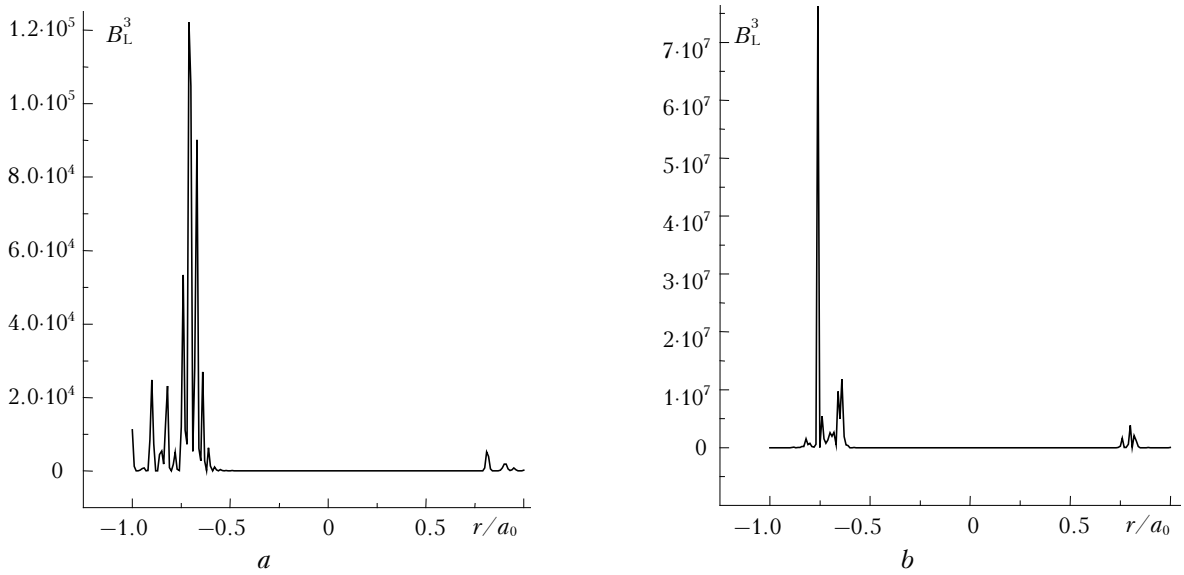

Fig. 7. Radial distribution of the pump field relative intensity along the principal diameter of ethanol drops with the radius of (*a*) 10 μm and (*b*) 50 μm in the case of three-photon excitation of fluorescence. The incidence direction of main radiation is from the right to the left.

It follows from Fig. 5 that with the increasing particle size the magnitude of V_m/V_a in the maximum of the forward zone decreases, while in the maximum of the rear zone this ratio increases, which is indicative of the power increase of fluorescent sources in the dark hemisphere with the increase of the particle radius.

Figure 6 shows the ratio of the source field relative intensity in the zone of the rear and front maxima B^3_{Lr}/B^3_{Lf} as a function of the diffraction parameter x_a of ethanol drops at three-photon absorption.

The magnitude of B^3_{Lr}/B^3_{Lf} is maximal for small particles and decreases with the increasing particle size. This means that in large particles the internal optical field practically always is resonant, which leads to smoothing of the scattering phase function asymmetry in the forward and backward directions.

This fact is supported by Fig. 7, which shows the distribution of the pump field relative intensity in ethanol drops of different radii in the case of three-photon absorption in particles exposed to radiation with $\lambda = 0.8$ μm. It is seen from Fig. 7 that for large particles with $a_0 = 50$ μm the ratio B^3_{Lr}/B^3_{Lf} decreases 1.6 times as compared to the excitation of small particles.

Thus, our study revealed that the emitting source position in a particle significantly affects the scatter diagram. If the emission source lies on the optical axis near the dark surface, then the scatter diagram has a backward peak with respect to incident radiation. As the source displaces to the particle center, the asymmetry of the secondary radiation vanishes.

For one-photon absorption, the scattering phase function is close to symmetric in the forward/backward directions. For multiphoton processes, the emission source is mostly located near the particle's dark surface, which causes an asymmetry of the scattering phase function in the forward direction.

Acknowledgments

This work was supported, in part, by the Russian Foundation for Basic Research (grant No. 03–05–64228).

References

1. S.C. Hill, Y. Pan, S. Holler, and R.K. Chang, Phys. Rev. Lett. **85**, No. 1, 54–57 (2000).
2. V.O. Kobak, *Radar Reflectors* (Sov. Radio, Moscow, 1975), 248 pp.
3. Yu.E. Geints, A.A. Zemlyanov, and E.K. Panina (Chistyakova), Atmos. Oceanic Opt. **12**, No. 7, 575–581 (1999).
4. Yu.E. Geints, A.A. Zemlyanov, V.E. Zuev, A.M. Kabanov, and V.A. Pogodaev, *Nonlinear Optics of Atmospheric Aerosol* (SB RAS Publishing House, Novosibirsk, 1999), 260 pp.
5. M. Abramovitz and I.A. Stegun, *Handbook of Mathematical Functions with Formulas, Graphs, and Mathematical Tables* (Dover, New York, 1965).
6. Yu.E. Geints and A.A. Zemlyanov, in: *Proc. of XI Joint International Symposium on Atmospheric and Ocean Optics. Atmospheric Physics* (Tomsk, 2004), p. 97.